

Deep Learning for Channel Sensing and Hybrid Precoding in TDD Massive MIMO OFDM Systems

Kareem M. Attiah, *Graduate Student Member, IEEE*, Foad Sohrabi, *Member, IEEE*, and Wei Yu, *Fellow, IEEE*

Abstract—This paper proposes a deep learning approach to channel sensing and downlink hybrid beamforming for massive multiple-input multiple-output systems operating in the time division duplex mode and employing either single-carrier or multi-carrier transmission. The conventional precoding design involves estimating the high dimensional channel and designing the precoders based on such estimate. This two-step process is, however, not necessarily optimal. This paper shows that by training the analog sensing and designing the hybrid downlink precoders directly from the received pilots without the intermediate high-dimensional channel estimation, the overall system performance can be significantly improved. However, the direct approach that simultaneously designs the hybrid precoders is difficult to train and only works for a fixed number of users. In this paper, we develop a simplified semi-direct approach that enjoys most of the advantages of the direct design while eliminating its drawbacks. Specifically, the proposed approach learns the uplink sensing stage and downlink analog precoder using deep learning and designs the digital precoder based on an estimate of the low-dimensional equivalent channel. Numerical comparisons show that the proposed methodology requires significantly less training overhead than the conventional strategy and further demonstrate its generalizability to various different system settings.

Index Terms—Deep learning (DL), hybrid precoding, massive multiple-input multiple-output (MIMO), millimeter wave (mmWave), time division duplex (TDD).

I. INTRODUCTION

Millimeter wave (mmWave) communication has attracted significant interest as means of addressing the increasing demand for faster data rates in future cellular networks [2]–[4]. As compared to the traditional sub-30GHz communication bands, wireless transmissions at mmWave frequencies experience more severe path and penetration loss. Fortunately, the poor channel conditions of mmWave communications can be effectively mitigated through the use of massive multiple-input multiple-output (MIMO) antenna arrays [5]. However, despite the advantages of utilizing large antenna arrays, the practical deployment of the fully digital massive MIMO is hindered by the excessive power consumption associated with the large number of radio frequency (RF) chains. To overcome this limitation, several alternative solutions have been proposed to permit the use of large antenna arrays while reducing the high power consumption. In this paper, we focus on the so-called hybrid beamforming architecture [6], [7] wherein the fully digital beamformer is replaced by an analog beamformer that maps the received signal on the antennas into a small number

of RF chains using a network of phase shifters, followed by a low-dimensional digital beamformer.

This paper considers the problem of constructing the hybrid beamformers from imperfect channel state information (CSI) in massive MIMO systems for frequency-flat as well as frequency-selective propagation environments with a limited number of scatters. We focus on the time-division duplex (TDD) operation so that channel reciprocity can be exploited in order to efficiently acquire the CSI at the base station (BS) using uplink pilots [5]. The existing hybrid precoding strategies for TDD massive MIMO systems follow a two-step methodology that decomposes the overall precoding procedure into a channel sensing and estimation step followed by a subsequent downlink precoding step. In the channel sensing and estimation step, the spatial and frequency characteristics of the mmWave channel are often exploited to recover an estimate of the channel parameters, e.g., [8]–[11]. Then, in the downlink precoding step, the BS constructs the precoding matrices using algorithms that treat the estimated CSI as perfect CSI.

This work is motivated by the key observation that the above conventional paradigm is not necessarily optimal, especially in the short pilot regime. This is because the conventional channel estimation process typically uses specific distance metric, such as the square loss (possibly with a regularizer on the model parameters), without accounting for the effect of channel estimation errors in the subsequent precoding step. Consequently, such a metric may not exactly match the ultimate goal of maximizing the overall system performance (e.g., sum rate). The main point of this work is that by adopting an end-to-end design that directly constructs the hybrid precoders from the received pilots without the intermediate channel estimation step, we can overcome the drawbacks of the conventional precoding framework, thereby enhancing the overall system performance.

A. Main Contributions

This paper proposes a joint channel sensing and downlink precoding approach that bypasses explicit channel estimation. Driven by the success of deep learning in tackling intricate optimization problems, we advocate the use of a deep neural network (DNN) to model the end-to-end massive MIMO system encompassing channel sensing, estimation, and downlink precoding, and to learn a direct mapping for the hybrid precoding matrices. A main contribution of this paper is that we highlight the inherent limitation of the conventional channel estimation based precoding and demonstrate how a learning based strategy is well suited to bypass this limitation.

The authors are with The Edward S. Rogers Sr. Department of Electrical and Computer Engineering, University of Toronto, Toronto, ON M5S 3G4, Canada (e-mails: {kattiah, fsohrabi, weiyu}@ece.utoronto.ca). The materials in this paper have been presented in part at IEEE Global Communications Conference (GlobeCom) Workshop, Taipei, Taiwan, December 2020 [1]. This work is supported by Huawei Technologies Canada.

The first part of this work considers a frequency-flat mmWave propagation model. In this case, the precoding problem involves the design of the analog precoding matrix and a single digital precoding matrix. However, it turns out that using the naive learning approach that simultaneously learns the analog and digital precoders is infeasible due to high training complexity and the impractical requirement that the number of users remains fixed. To circumvent these limitations, we develop an alternative semi-direct strategy that bypasses explicit channel estimation for the analog part design. In particular, we decompose the uplink pilot training into analog and digital training phases in which we separately construct the respective precoding matrices. In the analog training phase, a DNN is employed to train the sensing matrices and to learn a direct mapping for the analog precoding matrix. The proposed DNN architecture decomposes across the users and is, therefore, amenable to a relatively simple training. Furthermore, to avoid the metric mismatch problem, the training of this DNN is performed so as to minimize a simplified loss function derived from the rate expression. Once the analog beamforming matrix is determined, the end-to-end hybrid precoding system can be transformed into a low-dimensional fully digital system, thus allowing the digital precoding matrix to be designed based on the estimated equivalent channel from a few additional pilots. Numerical results indicate that the proposed approach significantly outperforms the conventional framework that separates channel estimation and downlink precoding.

The second part of this paper is concerned with a frequency-selective propagation environment. In this case, the BS utilizes multi-carrier techniques, e.g., orthogonal frequency division multiplexing (OFDM), to transmit several data streams over different subcarriers. A major challenge in the design of hybrid precoders for OFDM systems is that the analog precoder is common to the channels across subcarriers, whereas the digital precoder is different for every subcarrier. This physical limitation suggests a different treatment for the analog and digital parts and can be seen as an additional motivation behind our initial choice to separate the designs of the analog and digital precoders. Specifically, such decoupling allows the previous semi-direct approach to have a natural extension in which we design the analog precoder using a DNN based on the received pilots on all subcarriers, and design the digital precoders for every subcarrier based on the corresponding estimated equivalent channel. Further, to ensure modest training complexity that does not grow with the number of subcarriers, we incorporate a convolutional stage in the neural network architecture. This convolutional stage offers dimensionality reduction and summarizes the information in correlated received pilots over different subcarriers.

In practice, a wireless environment is inherently non-static and the channel parameters are always changing. A major concern in using data-driven solutions in communication systems is how robust such solutions are to changes in system parameters. As such, this paper also investigates the generalizability of the proposed approach in different system parameters. We use experimental case studies for the number of channel paths, uplink signal-to-noise ratio (SNR), and number of users, to demonstrate the ability of the proposed scheme to maintain

good performance even when the training and test sets are different. Further, we also provide a realistic single-cell simulation and use a general utility function (e.g., weighted sum rate) as a means to measure the system-level performance. The numerical findings indicate that the proposed approach is able to provide fairness among the different users.

B. Related Works

Earlier works on hybrid precoding design typically assume full CSI knowledge at the BS. The main focus of these works is to devise low-complexity algorithms that can approach the performance of the fully digital massive MIMO system for both cases of single-carrier and OFDM transmissions. Most existing algorithms involve heuristic designs for the analog part and conventional linear precoding for the digital part. Examples of these analog heuristic designs include matching to the channel phases [12], [13], matching to the channel strongest path [14], and iterative coordinate ascent [15] for single-carrier systems as well as channel covariance averaging [16], [17] and time-domain matched filtering [18] for multi-carrier systems. Another interesting line of work is the presented in [19] in which the precoder for a fully digital system is decomposed into analog and digital precoders using alternating minimization.

In practice, the CSI is not readily available at the BS and it must be estimated. The most widely common approach for channel estimation is to take advantage of the sparsity of the mmWave channels in the angular domain [8]–[11], [20]. For the single-carrier setup, [8] develops a channel estimation algorithm inspired by the greedy orthogonal matching pursuit (OMP), while [9] presents a multi-resolution codebook design for channel sensing and parameter estimation. Further, the work in [10] formulates the channel estimation as a sparse recovery problem from noisy measurements, for which the generalized approximate message passing (AMP) is used to retrieve the channel parameters. For the multi-carrier setup, [20] develops a matching pursuit algorithm for environments with line-of-sight conditions, whereas [11] further exploits the frequency correlation of the channel across subcarriers to devise a low-complexity variant of the OMP, named simultaneous weighted OMP (SW-OMP).

Recently, deep learning has attracted significant interest in the wireless research community. In most hybrid precoding works, the domain of application for deep learning was only restricted to replacing key system components with a neural network. This includes replacing channel estimation [21]–[23], downlink precoding with the input being either perfect/imperfect CSI [24], [25], or both [26]. The main limitation of all these works is that they admit the traditional separation of channel estimation and precoding and do not exploit the ability of data-driven approaches to model the end-to-end system. We remark that several recent works have proposed the idea of bypassing channel estimation in related wireless communication settings in order to optimize some system-wide objective, e.g., for scheduling in ad-hoc networks [27], and for transmission design in systems involving intelligent reflective surfaces [28] and fully digital massive MIMO in frequency division duplex mode [29].

Finally, we note that the recent work [30] also proposes a hybrid precoding design from received pilots in OFDM systems using DNNs. However, [30] only considers a single user setup. In contrast, the work presented herein considers the more challenging multi-user setup where the hybrid precoders are designed in the presence of user interference. Further, unlike the approach in [30], the proposed method constructs the analog and digital precoders separately. As a result, the proposed DNN is easier to train and maintains roughly the same computational complexity regardless of the number of subcarriers. This makes the proposed approach well suited for OFDM systems with a large number of subcarriers.

C. Paper Organization and Notation

The rest of the paper is organized as follows. Section II presents the massive MIMO system model with hybrid architecture in its most general form as an OFDM system assuming a frequency-selective propagation environment. Section III considers the special case of a single-carrier setup and develops the proposed semi-direct approach that bypasses explicit channel estimation for the analog precoding design. We then discuss the extension of the proposed approach to the multi-carrier setup in Section IV. In Section V, we provide extensive numerical simulations that demonstrate the performance of the proposed precoding approach and examine its generalizability aspects. Finally, conclusions are drawn in Section VI.

This paper uses lower case boldface letters, and upper case boldface letters denote scalars, vectors, and matrices, respectively. We use $[\cdot]_i$, $[\cdot]_{ij}$ to denote the i -th element of a vector and the element in the i -th row and j -th column of a matrix. Furthermore, \otimes is the Kronecker product operator and $(\cdot)^H$ denotes the Hermitian transpose of matrices. The operators $|\cdot|$, $\log_2(\cdot)$, $\mathbb{E}[\cdot]$, and $\text{Tr}(\cdot)$ represent the absolute value, binary logarithm, expectation, and trace, respectively. Finally, \mathbf{I}_M , $\mathbf{0}$ are the identity matrix of size M and the all-zero matrix, respectively.

II. PRELIMINARIES AND SYSTEM MODEL

A. System Model

Consider a TDD massive MIMO system operating in a frequency-selective mmWave environment in which a BS with M antennas and $N_{\text{RF}} < M$ RF chains employs OFDM transmission over N_c subcarriers to serve K single-antenna users. Since the number of RF chains at the BS is limited, downlink precoding is split between the analog and digital domains. Specifically, let $s_k[j]$ be the intended symbol for user k over subcarrier j . To send a downlink data stream of symbols $\mathbf{s}[j] = [s_1[j], \dots, s_K[j]]^T$, the BS precodes the symbol vector $\mathbf{s}[j]$ using a per-subcarrier digital precoder $\mathbf{V}_D[j] \in \mathbb{C}^{N_{\text{RF}} \times K}$, $\forall j$. Then, it appends a cyclic prefix of length $L_{\text{CP}} > d_{\text{max}}$, where d_{max} is the maximum delay spread of the channel, and subsequently applies an inverse fast Fourier transform (IFFT) operation. Finally, the BS employs a wide-band analog precoding matrix $\mathbf{V}_{\text{RF}} \in \mathbb{C}^{M \times N_{\text{RF}}}$. Note that because the analog stage takes place after the IFFT module, we cannot design the analog matrix on a per subcarrier basis. In addition, since the analog precoding stage is typically

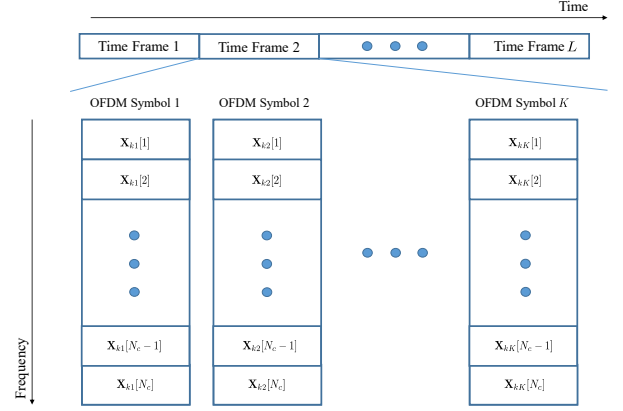


Fig. 1: The orthogonal uplink pilot scheme shown for the k -th user. To simplify the notation in the figure, we adopt $\mathbf{X}_{mn}[j]$ to denote the element of $\mathbf{X}[j]$ in the m -th row and n -th column.

implemented using a network of phase shifters, the elements of \mathbf{V}_{RF} must satisfy a constant modulus constraint, i.e., $[\mathbf{V}_{\text{RF}}]_{mn} = e^{j\phi_{mn}}$, where j is the imaginary unit.

Upon receiving the signal, each user applies an FFT operation followed by cyclic prefix removal. Mathematically, the equivalent model is given by:

$$\begin{aligned} y_k[j] &= \mathbf{h}_k^H[j] \mathbf{V}_{\text{RF}} \mathbf{V}_D[j] \mathbf{s}[j] + n_k[j], \\ &= \mathbf{h}_k^H[j] \mathbf{V}_{\text{RF}} \mathbf{v}_{D_k}[j] s_k[j] \\ &\quad + \sum_{i \neq k} \mathbf{h}_k^H[j] \mathbf{V}_{\text{RF}} \mathbf{v}_{D_i}[j] s_i[j] + n_k[j], \end{aligned} \quad (1)$$

where $y_k[j]$ and $\mathbf{h}_k[j]$ are respectively the received signal and frequency-domain channel of user k at subcarrier j , $\mathbf{v}_{D_k}[j]$ is the k -th column of $\mathbf{V}_D[j]$, and $n_k[j] \sim \mathcal{CN}(0, \sigma^2)$ is the Gaussian noise. We impose a total power constraint on the transmitted signal by taking $\mathbb{E}[\mathbf{s}[j] \mathbf{s}[j]^H] = \mathbf{I}_K$ and $\|\mathbf{V}_{\text{RF}} \mathbf{V}_D[j]\|_F^2 \leq P_D$, where P_D is the per-subcarrier power budget in the downlink.

For such a system, the overall achievable downlink rate for user k is given by the sum of rates across subcarriers, i.e.,

$$R_k = \sum_{j=1}^{N_c} \log_2 \left(1 + \frac{|\mathbf{h}_k^H[j] \mathbf{V}_{\text{RF}} \mathbf{v}_{D_k}[j]|^2}{\sum_{i \neq k} |\mathbf{h}_k^H[j] \mathbf{V}_{\text{RF}} \mathbf{v}_{D_i}[j]|^2 + \sigma^2} \right). \quad (2)$$

The main objective in this paper is to design the hybrid matrices so as to maximize the sum rate $\sum_k R_k$. To accomplish this, the BS must obtain information about the user channels. In this paper, we assume that the BS has no prior knowledge of the channels, but it can acquire noisy measurements of the channels through a pilot phase. Further, we assume that channel reciprocity holds [31] and the downlink CSI can be acquired in the uplink direction in a TDD operation.

We adopt an uplink pilot training scheme that takes place over L time frames each spanning K OFDM symbols. In particular, during a single time frame, the users send orthogonal pilots given by the rows of the matrices $\mathbf{X}[1], \dots, \mathbf{X}[N_c]$ over the K OFDM symbols, where each pilot matrix is a $K \times K$ unitary matrix. Fig. 1 illustrates this pilot scheme for the k -th user. The pilot matrices have the form $\mathbf{X}[j] = e^{j\phi[j]} \mathbf{X}$ with randomly a chosen angle $\phi[j]$ and some wide-band $K \times K$ unitary matrix \mathbf{X} . This choice is made to simplify

the pilot design while ensuring that different pilot symbols are transmitted over different subcarriers, thereby avoiding practical OFDM-related issues, such as high peak-to-average power ratio.

Since the number of RF chains is limited, the BS senses the channel in the ℓ -th time frame using an analog sensing matrix $\mathbf{W}_{\text{RF}}^{(\ell)} \in \mathbb{C}^{N_{\text{RF}} \times M}$, where the matrix elements satisfy $[\mathbf{W}_{\text{RF}}^{(\ell)}]_{mn} = e^{j\psi_{mn}}$. The received $N_{\text{RF}} \times K$ signal matrix at the j -th subcarrier in the ℓ -th time frame is:

$$\mathbf{R}^{(\ell)}[j] = \sqrt{P_U} \mathbf{W}_{\text{RF}}^{(\ell)} \mathbf{H}[j] \mathbf{X}[j] + \mathbf{W}_{\text{RF}}^{(\ell)} \mathbf{N}^{(\ell)}[j], \quad (3)$$

where $\mathbf{H}[j] \triangleq [\mathbf{h}_1[j], \dots, \mathbf{h}_K[j]]$ and $\mathbf{N}^{(\ell)}[j]$ is the uplink noise. Moreover, P_U is the users' power budget per subcarrier in a single time frame. Upon receiving the pilots, the BS right-multiplies the received signal at the j -th subcarrier by $\mathbf{X}[j]^H$. Since $\mathbf{X}[j]$ is unitary, the resulting signal is:

$$\begin{aligned} \tilde{\mathbf{Y}}^{(\ell)}[j] &\triangleq [\tilde{\mathbf{y}}_1^{(\ell)}[j], \dots, \tilde{\mathbf{y}}_K^{(\ell)}[j]] \\ &= \sqrt{P_U} \mathbf{W}_{\text{RF}}^{(\ell)} \mathbf{H}[j] + \mathbf{Z}^{(\ell)}[j], \end{aligned} \quad (4)$$

where $\mathbf{Z}^{(\ell)}[j] \triangleq \mathbf{W}_{\text{RF}}^{(\ell)} \mathbf{N}^{(\ell)}[j] \mathbf{X}^H[j]$. Define $\mathbf{H}_k \triangleq [\mathbf{h}_k[1], \dots, \mathbf{h}_k[N_c]] \in \mathbb{C}^{M \times N_c}$ as the overall channel matrix for user k over the entire frequency band and

$$\tilde{\mathbf{Y}}_k \triangleq \begin{bmatrix} \tilde{\mathbf{y}}_k^{(1)}[1] & \dots & \tilde{\mathbf{y}}_k^{(1)}[N_c] \\ \vdots & \ddots & \vdots \\ \tilde{\mathbf{y}}_k^{(L)}[1] & \dots & \tilde{\mathbf{y}}_k^{(L)}[N_c] \end{bmatrix} \in \mathbb{C}^{LN_{\text{RF}} \times N_c} \quad (5)$$

as the aggregate received matrix for user k in L time frames over the entire frequency band. Based on (4), we can write:

$$\tilde{\mathbf{Y}}_k = \sqrt{P_U} \mathbf{W}_{\text{RF}} \mathbf{H}_k + \mathbf{Z}_k, \quad (6)$$

where $\mathbf{W}_{\text{RF}} \triangleq \left[\left(\mathbf{W}_{\text{RF}}^{(1)} \right)^T, \dots, \left(\mathbf{W}_{\text{RF}}^{(L)} \right)^T \right]^T$ is the overall sensing matrix in L time frames and \mathbf{Z}_k is the effective noise.

For the described system, the hybrid precoding design problem can be stated as follows. Given the noisy measurements $\{\tilde{\mathbf{Y}}_k\}_{k=1}^K$ obtained through the sensing matrix \mathbf{W}_{RF} at the BS, we seek to construct the analog and digital precoding matrices according to:

$$(\mathbf{V}_{\text{RF}}, \mathbf{V}_D[1], \dots, \mathbf{V}_D[N_c]) = \mathcal{F}(\tilde{\mathbf{Y}}_1, \dots, \tilde{\mathbf{Y}}_K), \quad (7)$$

so as to maximize the sum-rate expression, where $\mathcal{F}(\cdot)$ is a function that maps the received pilots into the hybrid precoding matrices. Mathematically, this can be expressed in terms of the following optimization problem:

$$\begin{aligned} &\underset{\mathbf{W}_{\text{RF}}, \mathcal{F}(\cdot)}{\text{maximize}} \quad \sum_{k=1}^K \sum_{j=1}^{N_c} \log_2 \left(1 + \frac{|\mathbf{h}_k^H[j] \mathbf{V}_{\text{RF}} \mathbf{V}_{D_k}[j]|^2}{\sum_{i \neq k} |\mathbf{h}_i^H[j] \mathbf{V}_{\text{RF}} \mathbf{V}_{D_i}[j]|^2 + \sigma^2} \right) \\ &\text{subject to} \quad (\mathbf{V}_{\text{RF}}, \mathbf{V}_D[1], \dots, \mathbf{V}_D[N_c]) = \mathcal{F}(\tilde{\mathbf{Y}}_1, \dots, \tilde{\mathbf{Y}}_K), \\ &\quad |\mathbf{W}_{\text{RF}}[mn]| = 1, \quad \forall m, n, \\ &\quad |\mathbf{V}_{\text{RF}}[m'n']| = 1, \quad \forall m', n', \\ &\quad \text{Tr}(\mathbf{V}_D^H[j] \mathbf{V}_{\text{RF}}^H \mathbf{V}_{\text{RF}} \mathbf{V}_D[j]) \leq P_D, \quad \forall j. \end{aligned} \quad (8)$$

Note that the overall sensing matrix \mathbf{W}_{RF} is incorporated in the above problem as an additional optimization variable.

This is because it serves the critical role of summarizing the information about the user channels, thereby directly affecting how well the precoding matrices are constructed. We remark that solving the optimization problem in (8) directly using conventional optimization based methods is challenging due to the non-convexity of the objective and constraints. Accordingly, the traditional precoding schemes seek to heuristically solve this problem by adopting a two-step process in which the user channels are first estimated and the downlink precoding matrices are subsequently designed based on the estimated channels. We demonstrate in the next section that this approach is far from optimal and it is advantageous to bypass the channel estimation step and directly determine the precoding matrices from the received pilots.

B. Channel Model

The mmWave environment is modeled as a frequency-selective channel. In particular, the channel of the k -th user at the j -th subcarrier is expressed as the N_c -point discrete Fourier transform of its impulse response:

$$\mathbf{h}_k[j] = \sum_{n=0}^{N_c} \mathbf{r}_k[n] e^{-j \frac{2\pi j n}{N_c}} = \sum_{n=0}^{d_{\max}} \mathbf{r}_k[n] e^{-j \frac{2\pi j n}{N_c}}, \quad (9)$$

where $\mathbf{r}_k[n]$ is the discrete-time impulse response of the channel for user k at time index n and the second equality follows from the assumption that the channel response has a maximum delay spread d_{\max} . Further, we assume that the discrete-time channel response follows a sparse model as the sum of L_p dominant paths. Accounting for the effects of pulse shaping [11], we have:

$$\mathbf{r}_k[n] = \frac{1}{\sqrt{L_p}} \sum_{\ell=1}^{L_p} \alpha_{\ell,k} p_{\text{rc}}(nT_s - \tau_{\ell,k}) \mathbf{a}_t(\theta_{\ell,k}, \phi_{\ell,k}), \quad (10)$$

where T_s denotes the sampling period, $p_{\text{rc}}(\cdot)$ denotes the normalized raised cosine pulse-shaping filter (i.e., $p_{\text{rc}}(0) = 1$), and for simplicity L_p is assumed to be the same for all users. In addition, $\alpha_{\ell,k} \sim \mathcal{CN}(0, 1)$ is the complex path gain, $\tau_{\ell,k}$ is the path delay, $\theta_{\ell,k}$ and $\phi_{\ell,k}$ are the uniformly distributed angles of departure (AoDs) in the elevation and azimuth, and $\mathbf{a}_t(\cdot, \cdot)$ denotes the array response vector. Throughout the paper, we assume that the BS is equipped with a two-dimensional uniform planar array (UPA) with M_h and M_v antennas in the horizontal and vertical directions, with $M = M_h M_v$. Moreover, the antenna separations in both directions are Δ_h and Δ_v , where $\Delta_h = \Delta_v = \Delta$. The array response vector for such configuration is given by [32]:

$$\mathbf{a}_t(\theta, \phi) = \mathbf{a}_h(\theta, \phi) \otimes \mathbf{a}_v(\phi), \quad (11)$$

where $\mathbf{a}_h(\cdot, \cdot)$ and $\mathbf{a}_v(\cdot)$ are respectively the array response vectors of a uniform linear array in the horizontal and vertical directions, i.e.,

$$\begin{aligned} \mathbf{a}_h(\theta, \phi) &= \left[1, e^{j \frac{2\pi}{\lambda} \Delta \cos(\phi) \sin(\theta)}, \dots, e^{j \frac{2\pi}{\lambda} \Delta (M_h - 1) \cos(\phi) \sin(\theta)} \right]^T, \\ \mathbf{a}_v(\phi) &= \left[1, e^{j \frac{2\pi}{\lambda} \Delta \sin(\phi)}, \dots, e^{j \frac{2\pi}{\lambda} \Delta (M_v - 1) \sin(\phi)} \right]^T, \end{aligned}$$

and λ is the wavelength.

III. HYBRID PRECODING DESIGN FOR FREQUENCY-FLAT SINGLE-CARRIER SYSTEMS

To fix ideas and gain more insight, we begin by considering the simpler problem of hybrid precoding design in single-carrier systems. For a single-carrier mmWave massive MIMO system, the hybrid precoding problem entails the design of the analog precoding matrix $\mathbf{V}_{\text{RF}} \in \mathbb{C}^{M \times N_{\text{RF}}}$ and a single digital precoding matrix $\mathbf{V}_{\text{D}} \in \mathbb{C}^{N_{\text{RF}} \times K}$. The uplink baseband received signal $\tilde{\mathbf{y}}_k \in \mathbb{C}^{L N_{\text{RF}}}$ for each user is given by:

$$\tilde{\mathbf{y}}_k = \sqrt{P_U} \mathbf{W}_{\text{RF}} \mathbf{h}_k + \mathbf{z}_k, \quad (12)$$

where \mathbf{h}_k is the channel vector and $\mathbf{z}_k \sim \mathcal{CN}(\mathbf{0}, \mathbf{W}_{\text{RF}} \mathbf{W}_{\text{RF}}^H)$ is the effective Gaussian noise for user k . As a result, the optimization in (8) boils down to:

$$\begin{aligned} & \underset{\mathbf{W}_{\text{RF}}, \mathbf{F}(\cdot)}{\text{maximize}} && \sum_{k=1}^K \log_2 \left(1 + \frac{|\mathbf{h}_k^H \mathbf{V}_{\text{RF}} \mathbf{V}_{\text{D}}|^2}{\sum_{i \neq k} |\mathbf{h}_k^H \mathbf{V}_{\text{RF}} \mathbf{V}_{\text{D}}|^2 + \sigma^2} \right) \\ & \text{subject to} && (\mathbf{V}_{\text{RF}}, \mathbf{V}_{\text{D}}) = \mathcal{F}(\tilde{\mathbf{y}}_1, \dots, \tilde{\mathbf{y}}_K), \\ & && |[\mathbf{W}_{\text{RF}}]_{mn}| = 1, \quad \forall m, n, \\ & && |[\mathbf{V}_{\text{RF}}]_{m'n'}| = 1, \quad \forall m', n', \\ & && \text{Tr}(\mathbf{V}_{\text{D}}^H \mathbf{V}_{\text{RF}}^H \mathbf{V}_{\text{RF}} \mathbf{V}_{\text{D}}) \leq P_{\text{D}}. \end{aligned} \quad (13)$$

Moreover, a narrow-band frequency-flat channel is adopted in this case by setting $d_{\text{max}} = 0$. In this case, $\tau_{\ell,k} = 0$ and the channel for the k -th user is given by:

$$\mathbf{h}_k \triangleq \mathbf{r}_k[0] = \frac{1}{\sqrt{L_p}} \sum_{\ell=1}^{L_p} \alpha_{\ell,k} \mathbf{a}_t(\theta_{\ell,k}, \phi_{\ell,k}). \quad (14)$$

We now discuss the motivation behind the proposed approach.

A. Motivation

The hybrid precoding problem in (13) is non-trivial to solve, because the objective and some constraints are non-convex. The conventional precoding methods are model-based techniques that decompose (13) into more tractable problems whose solutions can be obtained using standard optimization tools. In principle, some channel model is first assumed and the model parameters are then estimated. Subsequently, an estimate of the user channels is reconstructed and the rate maximizing downlink precoding matrices are obtained based on the estimated channels. To perform the channel estimation step, this conventional paradigm needs to introduce a metric to measure the distance between the true channel and the estimated counterpart. The hope is that by minimizing such a distance metric, the estimated channel would accurately approximate the true channel and accordingly good precoding matrices can be constructed in the subsequent step. The problem is, however, such that a metric can only be applied to the assumed channel model. Further, it is difficult to take into account the effect of the channel estimation error on the subsequent precoding step. A consequence of this is that minimizing such metric (e.g., square loss with possibly a regularizer on the model parameter) in the channel recovery step may not exactly match the ultimate goal of maximizing the system performance (i.e., the sum rate). We argue that this possible mismatch in design metric is the main limitation of

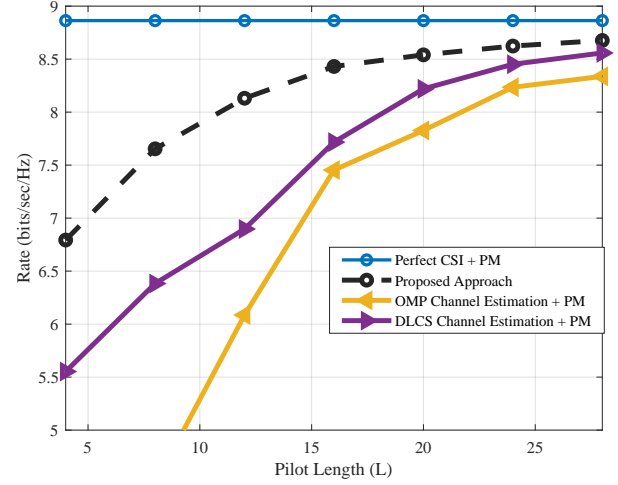


Fig. 2: Performance comparison of a single-carrier single user system. We set $M = 64$, $N_{\text{RF}} = K = 1$, and uplink/downlink SNR = 10dB.

the conventional design, but is otherwise necessary to ensure that the conventional design problem is tractable.

The advent of data-driven techniques shifts the paradigm toward a new possibility. Specifically, it is no longer necessary to adhere to the previous separation of channel recovery and downlink precoding, i.e., it may be beneficial to bypass the explicit CSI estimation altogether and to directly design the hybrid precoders from the baseband received pilots. In other words, because of the power of DNN as a universal function approximator, it is now possible to pursue an end-to-end design encompassing both channel sensing/estimation and hybrid precoding. To illustrate the preceding concepts and to quantify the impact of metric mismatch that may arise due to channel estimation, we compare the performance of different precoding schemes in the simple scenario where $K = N_{\text{RF}} = 1$. We choose this simple case here since the interference term vanishes and the digital beamformer reduces to a scalar whose value can be predetermined based on the downlink power budget P_{D} . Further, the rate maximizing analog precoder has a simple optimal structure that we denote by phase matching (denoted as “PM” in the figures) [13]. This comparison is shown in Fig. 2. The proposed precoding scheme is a data-driven approach that maps the received pilots directly into the analog precoding vector¹. The two remaining schemes estimate the channel parameters using the OMP [8] or a neural network [26] and subsequently apply phase matching on the estimated channels. From this figure, we can observe sizable gain due to bypassing channel estimation. We emphasize that such gain manifests itself when the resources for CSI acquisition are limited, e.g., when the pilot length is short. For sufficiently long pilot lengths, accurate channel estimation is possible and the conventional channel recovery based schemes can approach the direct design.

The discussion so far highlights the advantage of the direct design of the hybrid precoding matrices and advocates the use of data-driven approaches to undertake this task. However, our numerical experiments suggest that a direct attack on the multi-user hybrid precoding problem in (13) using a data-

¹The implementation details will be described in Section III-B.

driven approach is cumbersome. To see this, consider a naive implementation in which we seek to learn the mapping $\mathcal{F}(\cdot)$ directly using a DNN². Let Θ be the parameter set of the DNN architecture that models this downlink precoding system, the sum rate optimization problem can now be stated as follows:

$$\begin{aligned} & \underset{\Theta}{\text{minimize}} \quad \mathbb{E} \left[\sum_{k=1}^K R_k \right] \\ & \text{subject to} \quad (\mathbf{V}_{\text{RF}}, \mathbf{V}_{\text{D}}) = \mathcal{F}_{\text{NN}}(\tilde{\mathbf{y}}_1, \dots, \tilde{\mathbf{y}}_K; \Theta), \end{aligned} \quad (15)$$

where $\mathcal{F}_{\text{NN}}(\cdot; \Theta)$ represents the input-output relationship of the DNN and the expectation is taken over the channel and noise distributions. We can learn the DNN parameters by replacing the expectation with the empirical average over some training set \mathcal{T} and subsequently employing a stochastic gradient descent (SGD) algorithm.

While it is easy to see that this method bypasses the channel-recovery step and avoids the limitations of the traditional precoding scheme, it turns out that such an approach suffers from a number of drawbacks. First, the training process is severely hindered by complexity due to the multiplicative interaction between the analog and digital precoding matrices. Second, note that the input and output dimensions of this DNN depend on the number of users. Hence, such a method works under the assumption that the number of users is fixed. This implies that a different DNN needs to be trained every time the number of served users changes. Thus, this naive approach is difficult to implement in practice, and an alternative learning strategy is needed.

B. Proposed Precoding Design

This section develops the proposed semi-direct data-driven scheme that overcomes the limitation of channel recovery based approaches while enabling simpler training and better generalizability than the aforementioned naive application of the DNN. The key idea behind the proposed approach is two-fold. First, we decouple the design of the analog and digital precoding stages and learn a direct mapping for the analog precoder only. Consequently, the training complexity of the DNN that learns this mapping is manageable. Second, we decompose the overall DNN architecture into several *per-user DNNs*, each outputting one column of \mathbf{V}_{RF} . This has the benefit that the input and output dimensions of the per-user DNNs no longer depend on K , thereby allowing the proposed approach to be generalizable to systems with any number of users.

In order to decouple the design of \mathbf{V}_{RF} and \mathbf{V}_{D} , we split the overall pilot training phase of L frames into an analog training phase of L_a frames and a digital training phase of L_d frames with $L = L_a + L_d$. In the analog training phase, the received pilots in the first L_a frames are mapped directly into the analog precoding matrix. Then, in the digital training phase, we fix the analog beamformers and obtain the digital precoding based on the pilots received in the remaining L_d frames. The block diagram of the overall proposed scheme is shown in Fig. 3.

²For simplicity, we assume in this example that the analog sensing matrix \mathbf{W}_{RF} is given. Hence, the task is reduced to that of learning $\mathcal{F}(\cdot)$ only.

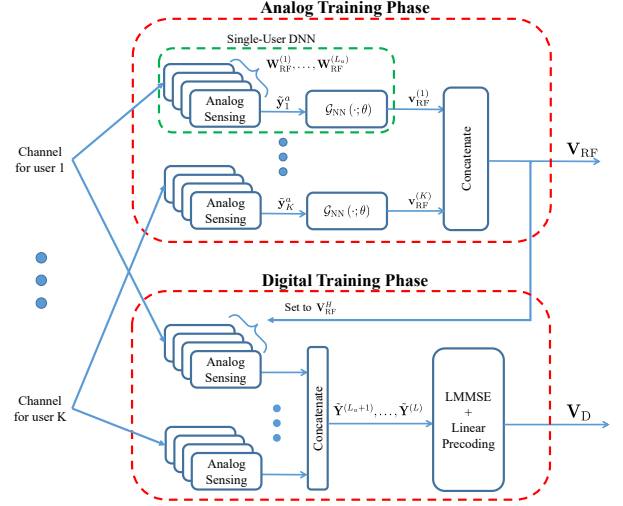


Fig. 3: Block diagram of the proposed precoding approach for designing the analog and digital precoding matrices in a single-carrier TDD MIMO system.

C. Analog Training Phase

We assume that $K = N_{\text{RF}}$ so that \mathbf{V}_{RF} has K columns. This assumption is typically made in most hybrid precoding works [13], [26], [33] due to the practical importance of this fully loaded case. Let us denote the received pilot from the k -th user in the first L_a time frames by $\tilde{\mathbf{y}}_k^a \triangleq \left[(\tilde{\mathbf{y}}_k^{(1)})^T, \dots, (\tilde{\mathbf{y}}_k^{(L_a)})^T \right]^T$, then using (12), we may write:

$$\tilde{\mathbf{y}}_k^a = \sqrt{P_U} \mathbf{W}_{\text{RF}}^a \mathbf{h}_k + \mathbf{z}_k^a, \quad (16)$$

where $\mathbf{W}_{\text{RF}}^a \triangleq \left[(\mathbf{W}_{\text{RF}}^{(1)})^T, \dots, (\mathbf{W}_{\text{RF}}^{(L_a)})^T \right]^T$ and \mathbf{z}_k^a is the corresponding Gaussian noise.

In the analog training phase, we seek to determine the analog precoder directly from the received pilots in (16) using a DNN on a per-user basis. To accomplish this, we decompose the overall DNN architecture into K non-interconnected branches. In the k -th branch, we have a single user DNN (SU-DNN), with parameters Θ_k , that determines the k -th analog precoding vector $\mathbf{v}_{\text{RF}}^{(k)}$ from $\tilde{\mathbf{y}}_k^a$ using the following direct mapping:

$$\mathbf{v}_{\text{RF}}^{(k)} = \mathcal{G}_{\text{NN}}(\tilde{\mathbf{y}}_k^a; \Theta_k), \quad \forall k. \quad (17)$$

The goal is to find the DNN parameters in each branch Θ_k and the sensing matrix \mathbf{W}_{RF}^a so that some average loss function is minimized:

$$\begin{aligned} & \underset{\mathbf{W}_{\text{RF}}^a, \{\Theta_k\}_{k=1}^K}{\text{minimize}} \quad \mathbb{E}[\mathcal{L}(\mathbf{V}_{\text{RF}})] \\ & \text{subject to} \quad \mathbf{v}_{\text{RF}}^{(k)} = \mathcal{G}_{\text{NN}}(\sqrt{P_U} \mathbf{W}_{\text{RF}}^a \mathbf{h}_k + \mathbf{z}_k^a; \Theta_k), \quad \forall k. \end{aligned}$$

Strictly speaking, since the ultimate goal is sum rate maximization, the loss function should be defined in terms of the maximum sum rate expression taken over all choices of the digital precoder. In other words, for a given \mathbf{V}_{RF} , the loss function can be found by solving the optimization problem:

$$\mathcal{L}^{\text{opt}}(\mathbf{V}_{\text{RF}}) = \underset{\mathbf{V}_{\text{D}}: \|\mathbf{V}_{\text{RF}} \mathbf{V}_{\text{D}}\|_F^2 \leq P_D}{\text{maximize}} \quad \sum_{k=1}^K R_k. \quad (18)$$

However, this is a non-convex problem; further such a loss function introduces coupling across the users. Instead, we seek to find an alternative loss function that approximates the actual sum rate while allowing for relatively simple training. Toward this end, we make an assumption that the interference terms can be ignored in the analog part design. This is because the subsequent digital precoder is typically designed to alleviate the effect of interference, e.g., using zero forcing (ZF). Therefore, during the analog part design, we can approximate each user's achievable rate based on its analog beamforming gain without taking interference into account. Specifically, the proposed loss function is given by:

$$\mathcal{L}(\mathbf{V}_{\text{RF}}) = - \sum_{k=1}^K \log_2 \left(1 + \frac{P_D}{MK\sigma^2} |\mathbf{h}_k^H \mathbf{v}_{\text{RF}}^{(k)}|^2 \right). \quad (19)$$

Since the loss function (19) consists of K independent terms each of which is a function of a single analog precoding vector $\mathbf{v}_{\text{RF}}^{(k)}$, the training process is considerably simplified. To see this, let us first assume that the sensing matrix \mathbf{W}_{RF}^a is given. It can be seen that the objective and the constraints are easily decoupled over the user. As such, the overall minimization problem is equivalent to performing K minimizations each over a given parameter set Θ_k for some k :

$$\begin{aligned} & \underset{\Theta_k}{\text{minimize}} \quad \mathbb{E} \left[-\log_2 \left(1 + \frac{P_D}{MK\sigma^2} |\mathbf{h}_k^H \mathbf{v}_{\text{RF}}^{(k)}|^2 \right) \right] \\ & \text{subject to} \quad \mathbf{v}_{\text{RF}}^{(k)} = \mathcal{G}_{\text{NN}}(\tilde{\mathbf{y}}_k^a; \Theta_k), \end{aligned}$$

where the expectation is taken over the distributions of the channel and the noise associated with the k -th user, i.e., \mathbf{h}_k , and \mathbf{z}_k . Hence, the overall training process can now be performed independently over the K branches of the DNN. We remark that the objective in the above optimization bears some similarity to that considered in [26], [33] for analog precoding design, which ultimately seeks to construct the analog precoding vectors to match the phases of the user channels. The key difference is that we instead construct the analog precoding vectors directly from the received pilots without the intermediate channel recovery step.

Next, we discuss how to jointly learn \mathbf{W}_{RF}^a and $\{\Theta_k\}$. It can be seen from (16) that \mathbf{W}_{RF}^a plays a similar role to a linear layer. Therefore, by adding a common linear layer with trainable weights at the front of each single user branch (see Fig. 3), we are able to incorporate the design of \mathbf{W}_{RF}^a in the DNN training.

To further facilitate training, we propose to tie the parameters of the SU-DNNs across the branches, i.e., set $\Theta_1 = \dots = \Theta_K = \Theta$. In this case, all the SU-DNNs become identical, i.e., they all have the same structure, same parameters, and same loss function. Consequently, training the overall DNN using a batch \mathcal{B} of independent channel realizations is now equivalent to training just one SU-DNN with K times as many channel samples taken column-wise from the elements of \mathcal{B} . The key advantage is that by employing K identical copies of the trained SU-DNN, we now arrive at a *generalizable* architecture suitable for systems with an arbitrary number of users. We emphasize here that this method is applicable even if the users

experience different channel distributions and different noise levels. This claim is numerically verified in Section V.

We remark that the analog precoder³ produced by the SU-DNNs has unrestricted angles. In practice, the analog stage is often implemented using finite-resolution phase shifters, which implies that the phases of the analog precoder take on values over a discrete set. A particular case of interest is when the entries of the analog precoding matrix are of the form:

$$[\mathbf{V}_{\text{RF}}]_{mn} = e^{j \frac{2\pi q}{Q}}, \quad \forall n, m,$$

where Q is an integer and $q = 0, \dots, Q-1$. To output the analog precoding matrix that adheres to this restriction, we first output the unrestricted analog precoding matrix using the pre-trained DNN architecture and subsequently round the angles to the nearest angle in the discrete set.

D. SU-DNN Architecture

The proposed SU-DNN that learns the analog sensing matrix \mathbf{W}_{RF}^a and the parameter set Θ is depicted in Fig. 4. This architecture consists of a sensing layer, a set of intermediate layers, and an entry-wise normalization layer.

1) *Sensing Layer*: The sensing stage can be regarded as a linear map with a transformation matrix given by \mathbf{W}_{RF}^a . The sensing layer is a linear trainable layer in the proposed architecture that models the analog sensing stage. The input of this layer is the user channel vector plus noise, whereas the output represents the corresponding received pilots. To enforce a unit modulus constraint on the layer weights, we define the phases of such weights as trainable parameters.

2) *Intermediate Layers*: The second stage consists of a cascade of intermediate layers that models the direct mapping from the received pilots \mathbf{y}_k^a to the unnormalized precoding vector $\tilde{\mathbf{v}}_k$. We consider an intermediate stage consisting of R layers, where each layer is fully connected with rectified linear unit (ReLU) activation, except for the last layer, which has linear activation. Mathematically, we have:

$$\tilde{\mathbf{v}}_k = \mathbf{W}_R \mathcal{R}(\dots \mathcal{R}(\mathbf{W}_1 \tilde{\mathbf{y}}_k^a + \mathbf{b}_1) \dots) + \mathbf{b}_R,$$

where $\mathcal{R}(\cdot) = \max(\cdot, 0)$ is the ReLU activation function and $\{\mathbf{W}_r, \mathbf{b}_r\}$ is the set of trainable parameters for layer r .

3) *Normalization Layer*: The output of the intermediate stage cannot be taken as the analog precoding vector since the entries of $\tilde{\mathbf{v}}_k$ do not satisfy the unit modulus constraint. The purpose of the normalization layer is to enforce this constraint on the elements of the output vector. This is accomplished by applying the normalization map $\mathcal{N}(x) \triangleq \frac{x}{|x|}$ component-wise on the elements of $\tilde{\mathbf{v}}_k$, i.e.,

$$[\mathbf{v}_{\text{RF}}^{(k)}]_i = \mathcal{N}([\tilde{\mathbf{v}}_k]_i), \quad \forall i. \quad (20)$$

In our prior work [1], we propose to output the phases of the analog precoding vector Φ_k in the intermediate stage and apply the component-wise exponential map $[\mathbf{v}_{\text{RF}}^{(k)}]_i = e^{j[\Phi_k]_i}$ in the subsequent layer to ensure that the analog constraint

³The discussion herein applies to both the analog precoding matrix as well as the analog sensing matrix. For simplicity, we restrict attention to the analog precoding matrix.

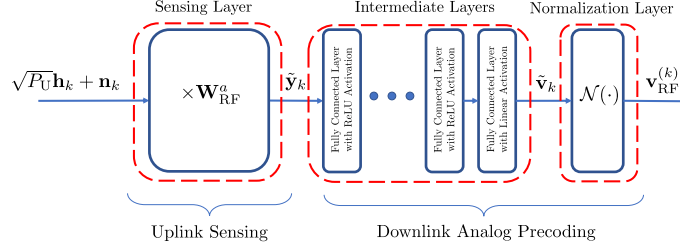


Fig. 4: The proposed SU-DNN for uplink sensing and downlink analog precoding design in single-carrier systems.

is met. However, our numerical experiments indicate that the normalization method (20) can achieve better performance.

4) *Training and Post-Training:* The training of the proposed DNN is performed offline in an unsupervised fashion to minimize the average loss function in (19). After training, we use the K copies of the SU-DNNs for operation wherein the sensing layer is used as the analog sensing matrix in the uplink pilot phase and the received pilot signal $\tilde{\mathbf{y}}_k^a$ is fed into the intermediate layers to produce the downlink analog precoder.

E. Digital Training Phase

In the digital training phase, we seek to design the digital precoder \mathbf{V}_D , given a predetermined \mathbf{V}_{RF} , based on the received pilots, where:

$$\tilde{\mathbf{Y}}^{(\ell)} = \sqrt{P_U} \mathbf{W}_{\text{RF}}^{(\ell)} \mathbf{H} + \mathbf{Z}^{(\ell)}, \quad \ell = L_a + 1, \dots, L. \quad (21)$$

We propose to construct the digital precoding using the traditional approach that separates the channel estimation and precoding modules since the performance loss due to the metric mismatch is negligible for low-dimensional channels.

For a fixed analog precoder, the low-dimensional equivalent channel seen by the digital precoder is $\mathbf{H}_{\text{eq}} = \mathbf{V}_{\text{RF}}^H \mathbf{H}$. To design \mathbf{V}_D , we compute an estimate of the equivalent channel $\hat{\mathbf{H}}_{\text{eq}}$ then use linear precoding to find \mathbf{V}_D from $\hat{\mathbf{H}}_{\text{eq}}$. The key idea is to set the analog sensing matrix to be the Hermitian of the analog precoding matrix, i.e.,

$$\mathbf{W}_{\text{RF}}^{(\ell)} = \mathbf{V}_{\text{RF}}^H, \quad \ell = L_a + 1, \dots, L, \quad (22)$$

so that $\hat{\mathbf{H}}_{\text{eq}}$ can be determined directly from the received pilots $\tilde{\mathbf{Y}}^{(L_a+1)}, \dots, \tilde{\mathbf{Y}}^{(L)}$ without having to estimate the high dimensional channel \mathbf{H} . To see this, note that (22) transforms the end-to-end massive MIMO system into a fully digital low-dimensional MIMO system whose channel is \mathbf{H}_{eq} . Indeed, by (22), the received pilots can now be expressed as:

$$\tilde{\mathbf{Y}}^{(\ell)} = \sqrt{P_U} \underbrace{\mathbf{V}_{\text{RF}}^H \mathbf{H}}_{\mathbf{H}_{\text{eq}}} + \mathbf{Z}^{(\ell)}, \quad \ell = L_a + 1, \dots, L. \quad (23)$$

The interpretation of (23) is that $\tilde{\mathbf{Y}}^{(L_a+1)}, \dots, \tilde{\mathbf{Y}}^{(L)}$ can now be regarded as repeated transmissions of the pilots through the equivalent channel. A key consequence is that this low-dimensional channel can be accurately estimated via the traditional linear minimum mean squared error (LMMSE) estimator of \mathbf{H}_{eq} using a relatively small number of transmissions. Assuming that the channels across the different antennas are

uncorrelated (i.e., $\mathbb{E}[\mathbf{h}_k \mathbf{h}_k^H] = \mathbf{I}_M, \forall k$), the LMMSE estimator for the equivalent channel is given by:

$$\hat{\mathbf{H}}_{\text{eq}} = \frac{\sqrt{P_U}}{P_U L_d + \sigma^2} \sum_{\ell=L_a+1}^L \tilde{\mathbf{Y}}^{(\ell)}. \quad (24)$$

In the foregoing discussion, the heuristic choice in (22) is motivated by the fact that it transforms the massive MIMO system into a low-dimensional fully digital system. Such a choice can also be theoretically justified for the special case of uncorrelated channels and $L_d = 1$, where it can be shown that this choice is optimal in the sense of minimizing the mean squared estimation error of the LMMSE estimator. However, we do not formally present this result here due to space limitations.

Having estimated \mathbf{H}_{eq} , we proceed to determine \mathbf{V}_D using conventional linear precoding schemes. Two common choices for digital precoding are ZF and the iterative weighted minimum mean squared error (WMMSE) [34]. For ZF, the digital precoder is $\mathbf{V}_D = \hat{\mathbf{H}}_{\text{eq}} (\hat{\mathbf{H}}_{\text{eq}}^H \hat{\mathbf{H}}_{\text{eq}})^{-1} \mathbf{D}_{\text{ZF}}$, where \mathbf{D}_{ZF} is the power allocation diagonal matrix. Despite its simplicity and its ability to mitigate interference, ZF suffers from noise enhancement. The WMMSE approach is an iterative strategy that reduces the combined effect of noise and interference. The WMMSE procedure for digital precoding design in hybrid systems is summarized in [16].

IV. HYBRID PRECODING DESIGN FOR FREQUENCY-SELECTIVE OFDM SYSTEMS

We now turn our attention to the more general OFDM-based massive MIMO system. The extension of the proposed algorithm to the multi-carrier case should be made with the following considerations: (i) A common analog precoder should be designed for all channels over N_c subcarriers, and (ii) Digital precoding should be performed on a per-subcarrier basis.

As before we divide the overall pilot phase into an analog training phase of length L_a , in which the analog precoder is determined using a direct mapping from the baseband received pilots, and a digital training phase of length L_d that entails estimating the low-dimensional equivalent channel followed by linear precoding design. To ensure that a common analog beamformer is appropriately designed for the channels over the entire band, the SU-DNN is trained to learn a mapping from the baseband received pilots matrix over the entire frequency band (i.e., $\tilde{\mathbf{Y}}_k$ in (6) for the k -th user) into the corresponding analog precoding vector. Further, to ensure digital precoding takes place on a per-subcarrier basis, the

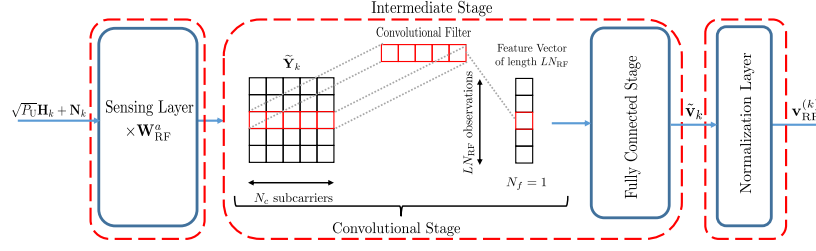


Fig. 5: The proposed SU-DNN for uplink sensing and downlink analog precoding design in multi-carrier systems. For simplicity, the operation of the convolution stage is shown when $N_f = 1$.

Algorithm 1: Hybrid Precoding for OFDM Systems

Input: Number of pilot time frames L_a , L_d , uplink and downlink powers P_U , P_D , noise variance σ^2 , pretrained sensing matrices in the analog precoding design phase $\{\mathbf{W}_{\text{RF}}^{(\ell)}\}_{\ell=1}^{L_a}$, and pretrained SU-DNN $\mathcal{G}_{\text{OFDM}}(\cdot; \boldsymbol{\Theta}_{\text{OFDM}})$.

Output: The analog precoder \mathbf{V}_{RF} , and the digital precoders $\mathbf{V}_D[1], \dots, \mathbf{V}_D[N_c]$.

Analog Precoding Design:

for $\ell = 1 \dots, L_a$ **do**

BS sets the analog sensing to $\mathbf{W}_{\text{RF}}^{(\ell)}$;

Users send pilots $\mathbf{X}[1], \dots, \mathbf{X}[N_c]$ across subcarriers over K OFDM symbols;

BS receives $\tilde{\mathbf{Y}}_k^{(\ell)} = \sqrt{P_U} \mathbf{W}_{\text{RF}}^{(\ell)} \mathbf{H}_k + \mathbf{Z}_k^{(\ell)}$;

end

for $k = 1 \dots, K$ **do**

BS constructs $\tilde{\mathbf{Y}}_k = \left[\left(\tilde{\mathbf{Y}}_k^{(1)} \right)^T, \dots, \left(\tilde{\mathbf{Y}}_k^{(L_a)} \right)^T \right]^T$;

BS computes $\mathbf{v}_{\text{RF}}^{(k)} = \mathcal{G}_{\text{OFDM}}(\tilde{\mathbf{Y}}_k; \boldsymbol{\Theta}_{\text{OFDM}})$;

end

BS determines $\mathbf{V}_{\text{RF}} = [\mathbf{v}_{\text{RF}}^{(1)}, \dots, \mathbf{v}_{\text{RF}}^{(K)}]$;

Digital Precoding Design:

BS sets the analog sensing matrix to \mathbf{V}_{RF}^H ;

for $\ell = L_a + 1 \dots, L$ **do**

Users send pilots $\mathbf{X}[1], \dots, \mathbf{X}[N_c]$ across subcarriers over K OFDM symbols;

BS receives

$$\tilde{\mathbf{Y}}_k^{(\ell)} = [\tilde{\mathbf{y}}_k^{(\ell)}[1], \dots, \tilde{\mathbf{y}}_k^{(\ell)}[N_c]] = \sqrt{P_U} \mathbf{V}_{\text{RF}}^H \mathbf{H}_k + \mathbf{Z}_k^{(\ell)};$$

end

for $j = 1 \dots, N_c$ **do**

BS forms $\tilde{\mathbf{Y}}^{(\ell)}[j] = [\tilde{\mathbf{y}}_1^{(\ell)}[j], \dots, \tilde{\mathbf{y}}_K^{(\ell)}[j]]$, $\forall \ell$;

BS determines the LMMSE estimate

$$\hat{\mathbf{H}}_{\text{eq}}[j] = \frac{\sqrt{P_U}}{P_U L_d + \sigma^2} \sum_{\ell=L_a+1}^L \tilde{\mathbf{Y}}^{(\ell)}[j];$$

BS determines $\mathbf{V}_D[j]$ using ZF or WMMSE on $\hat{\mathbf{H}}_{\text{eq}}[j]$.

end

low-dimensional channel for each subcarrier is estimated and the corresponding digital precoder is subsequently determined using linear precoding. The details of the proposed scheme are provided in Algorithm 1.

Analogous to the SU-DNN for the single-carrier case, the network architecture in the OFDM case consists of a sensing

layer, an intermediate stage and a normalization layer. The main difference is that the DNN in the OFDM case is designed to map the received pilots across all frequencies into a single analog precoder. To accomplish this, we propose an intermediate stage consisting of a convolutional layer followed by a fully connected stage. We utilize a convolutional layer to reduce the input dimension and exploit the correlation between the pilot measurements over different subcarriers, thereby reducing the computational complexity of the subsequent fully connected stage. In particular, we apply $N_f < N_c$ convolutional filters to the columns of the received pilot matrix $\tilde{\mathbf{Y}}_k$, where each convolutional filter is a 1-D horizontal stripe with length N_c and trainable parameters. Each filter output is then followed by a ReLU activation. This produces a convolution output consisting of N_f feature vectors each of length LN_{RF} . The feature vectors are then mapped into the unnormalized precoding vector using the subsequent fully connected stage. The overall DNN architecture is illustrated in Fig. 5, where the sensing and normalization layers are analogous to their counterparts for the DNN of single-carrier systems. Finally, we use the following loss function:

$$\mathcal{L}(\mathbf{V}_{\text{RF}}) = - \sum_{k=1}^K \sum_{j=1}^{N_c} \log_2 \left(1 + \frac{P_D}{MK\sigma^2} \left| \mathbf{h}_k^H[j] \mathbf{v}_{\text{RF}}^{(k)} \right|^2 \right), \quad (25)$$

which generalizes the loss function (19).

V. NUMERICAL RESULTS

In this section, we evaluate the performance of the proposed hybrid precoding scheme against existing benchmarks and investigate its ability to generalize in various system parameters.

A. Parameter Configuration and Implementation Details

We consider a massive MIMO system in TDD where the BS is equipped with $N_{\text{RF}} = 4$ RF chains and a two-dimensional UPA with $M_h = M_v = 8$. Thus, the total number of BS antennas is $M = 64$. The antenna separation in both directions is set to $\lambda/2$. For OFDM systems, the user channels follow the model introduced in Section II-B with $L_p = 4$ paths, a maximum delay spread $d_{\text{max}} = 4$, and $N_c = 128$ subcarriers. The channel paths are assumed to be independent and identically distributed (i.i.d) with complex Gaussian path gains $\alpha_{\ell,k} \sim \mathcal{CN}(0, 1)$ and uniform path delays $\tau_{\ell,k}$ over the interval $[0, d_{\text{max}} T_s]$, where $T_s = \frac{1}{1760} \mu\text{s}$ [11]. The azimuth and elevation AoDs follow a uniform distribution over the interval $[-\pi/2, \pi/2]$ and the pulse shaping filter is raised cosine with a roll-off factor of 0.8. For the single-carrier system, we adopt

the frequency-flat mmWave model introduced in Section III by setting $d_{\max} = 0$ and $N_c = 1$. Finally, we define the uplink SNR as $\text{SNR}_{\text{UL}} = 10 \log \frac{P_U}{\sigma^2}$ and the downlink SNR as $\text{SNR}_{\text{DL}} = 10 \log \frac{P_D}{\sigma^2}$.

We implement the proposed DNNs using TensorFlow [35]. Since most deep learning libraries do not support complex operations, we represent all complex quantities using their real representations and implement complex multiplications using real addition and multiplication. We set the number of fully connected intermediate layers of the single-carrier/OFDM SU-DNNs to $R = 3$, with dense layers of widths 1024, 512, and 256, respectively. For faster convergence, each dense layer is preceded by a batch normalization layer. In addition, for the OFDM neural network, we set the number of convolutional filters $N_f = 16$, which leads to a dimensionality reduction of the input space by a factor of 8 for a system with $N_c = 128$. We train the models using Adam optimizer [36]. The training was performed on minibatches of size 500 over many (~ 1000) epochs. The learning rate is initialized at 10^{-3} and progressively decreased by a factor of 2 every 100 epochs. We assume full knowledge of the channel and noise distributions so we can generate as many data samples as needed for training. Finally, we use a validation set of size 1000 to monitor the performance and keep the model parameters that achieved the best generalization.

B. Sum Rate Performance

We first analyze the performance of the proposed hybrid precoding scheme which bypasses the channel estimation step for the analog part design in a multi-user setup with $K = 4$ users and $\text{SNR}_{\text{UL}} = \text{SNR}_{\text{DL}} = 10\text{dB}$. In Fig. 6(a), we plot the sum rate against the number of pilot frames L assuming a single-carrier mmWave massive MIMO setup. For the proposed approach, we indicate the values of L_a and L_d on the figure. As benchmarks, we consider downlink precoding using phase matching [13] for the analog part and ZF for the digital part using perfect/imperfect CSI. The channel recovery based schemes used in the imperfect CSI case are the OMP algorithm [8] and the deep learning compressed sensing (DLCS) approach [26]. It can be seen in Fig. 6(a) that the proposed scheme significantly outperforms channel recovery based counterparts. For example, the proposed approach with $L = 8$ achieves over 85% of the total sum rate of the full CSI systems, while the DLCS does so with $L = 10$. This indicates over 20% saving in pilot overhead relative to the conventional channel recovery based schemes. This supports our main claim that the performance of the hybrid precoding system can be enhanced by bypassing explicit channel estimation for the analog part design. Further, we note that the pilot overhead needed for accurately estimating the low-dimensional channel and constructing the digital precoder is rather short. As noted earlier, this is typically the case since the equivalent channel is low-dimensional. Finally, we observe that the effect of optimizing the channel sensing matrix is noticeable only at a very short pilot length.

Next, we consider the same comparison for the multi-carrier setup. This comparison is shown in Fig. 6(b). For

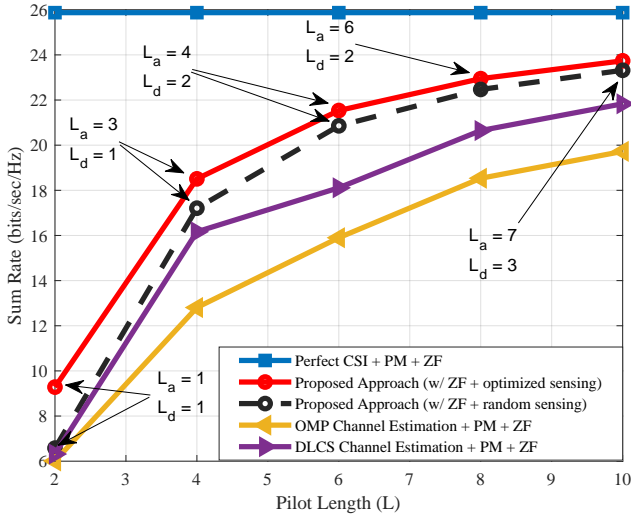
the baselines, we perform channel estimation according to SW-OMP [11] and the data-driven LAMP network [23], and utilize the covariance based scheme [16] for analog precoding and WMMSE for digital precoding. From Fig. 6(b), we can again observe that the performance of the proposed data-driven scheme is superior to the channel recovery based ones. Further, we also plot the sum rate of the proposed precoding approach assuming finite-resolution phase shifters. We observe that the performance of the proposed approach with only 2-bit phase shifters can already exceed the performance of the channel recovery based approaches with infinite-resolution phase shifters. Moreover, the performance of the proposed method with 3-bit phase shifters already approaches that of the infinite-resolution counterpart.

C. Generalizability Results

In this section, we seek to examine how well the system performs under parameter settings other than the ones used for training. This is crucial because wireless communication systems are typically far from static and their parameters constantly change over time. The main goal of this section is to show that the proposed data-driven scheme can maintain a robust operation against variations in system parameters.

First, we investigate the generalizability of the proposed scheme in the number of paths. To this end, we consider two scenarios for the proposed approach. In the first scenario, the DNN is trained and tested using datasets generated from the same distribution. This experiment is repeated for different values of the number of paths, i.e., $L_p \in \{2, \dots, 8\}$. Hence, this scenario represents the case where there is a perfect match in the distributions of the training and test sets. In the second scenario, we train the DNN using a training set with $L_p = 4$ and evaluate the performance on the test sets with $L_p \in \{2, \dots, 8\}$. We set $L_a = 6$ and $L_d = 2$ for the single-carrier setup and $L_a = 8$ and $L_d = 4$ for the multi-carrier setup. All other parameters remain similar to those given in Section V-B. We plot the sum rate against the number of paths in Fig. 7(a) for the single-carrier case and in Fig. 8(a) for the multi-carrier case. For comparison purposes, we also include the performance of the perfect CSI and OMP schemes for the single-carrier case, and SW-OMP for the multi-carrier case. It can be seen that there is no tangible loss in performance for the second scenario (i.e., in which a mismatch in L_p exists) relative to the first scenario (i.e., in which the numbers of paths for the training and test sets are equal). This indicates that the proposed DNN architecture is able to maintain a robust operation against variations in the number of channel paths.

Next, we numerically study the degradation in performance that may arise due to a mismatch in the uplink SNR. Analogous to the previous simulation, we consider two scenarios in this experiment. Specifically, in the first scenario the training and test sets are drawn from the same distribution and the uplink SNR is varied in the range of 0 – 20dB. Whereas in the second scenario, the training set is obtained by fixing the uplink SNR to 10dB. The results are shown in Fig. 7(b) for the single-carrier neural network and in Fig. 8(b) for the multi-carrier neural network. Once again, we see that there is only



(a) Single-carrier system.

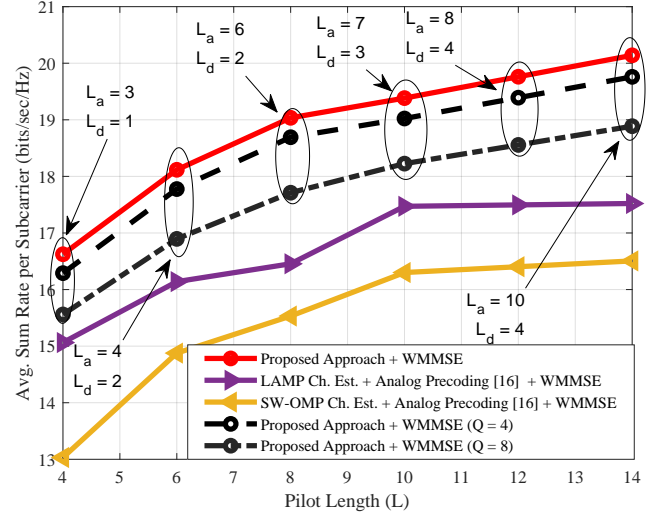
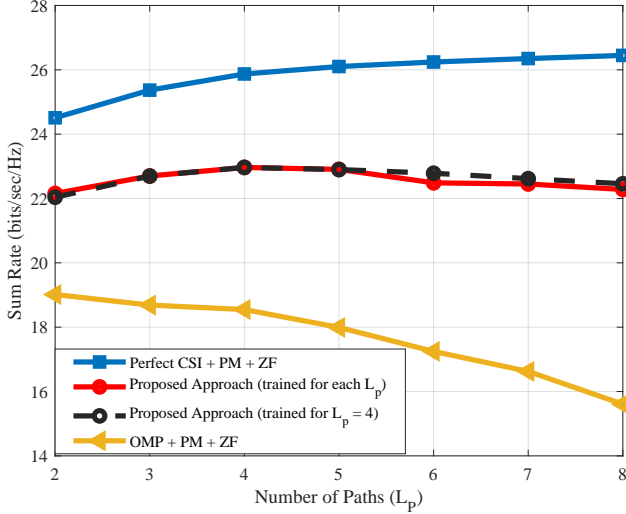
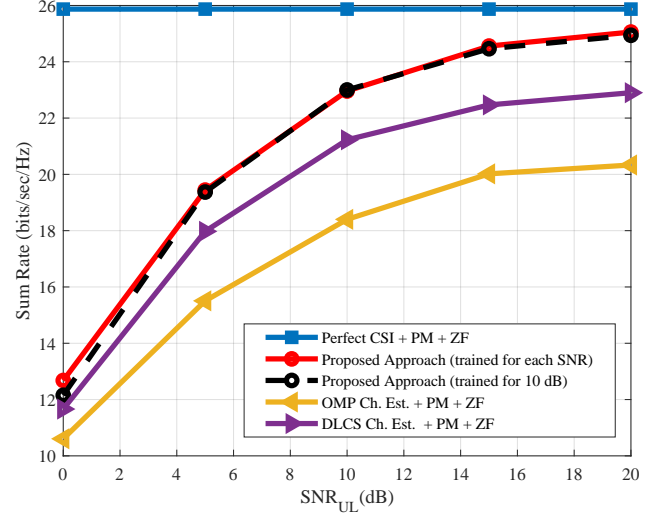
(b) Multi-carrier system with $N_c = 128$ subcarriers.

Fig. 6: Performance comparison (sum rate vs pilot length) of the proposed approach against existing schemes for different values of L when $K = N_{\text{RF}} = 4$ and $\text{SNR}_{\text{UL}} = \text{SNR}_{\text{DL}} = 10$ dB.



(a) Generalizability in the number of paths for the proposed scheme. We fix $\text{SNR}_{\text{UL}} = 10$ dB, and vary L_p from 2 to 8 paths.



(b) Generalizability in the uplink SNR for the proposed scheme. We fix $L_p = 4$, and vary SNR_{UL} from 0 to 20 dB.

Fig. 7: Generalizability of the single-carrier DNN in environment parameters. We set $N_{\text{RF}} = K = 4$, and $\text{SNR}_{\text{DL}} = 10$ dB.

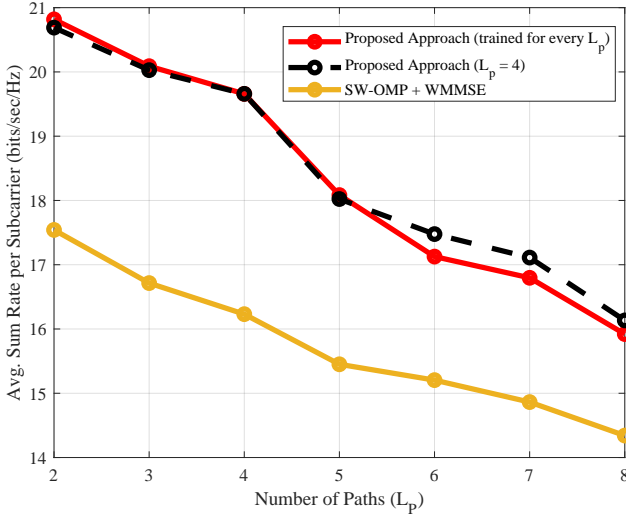
a negligible performance loss for the second scenario relative to the first one, thereby indicating that the proposed design is able to perform well even in the presence of variations in the uplink SNR.

Finally, we demonstrate the ability of the proposed approach to serve an arbitrary number of users. First, we study the case where all the users share the same channel distribution, the more general case in which the users do not share the same channel distribution is discussed in the next subsection. Thus, we train one single user neural network on the channel examples of all K users for the proposed scheme. After training, this SU-DNN is then duplicated across the K branches of the overall DNN. We examine the single-carrier case in Fig. 9(a) with $L = 3$, $L_a = 2$ and $L_d = 1$, and the multi-carrier case in Fig. 9(b) with $L = 7$, $L_a = 2$ and $L_d = 1$. In both simulations, we set $L_p = 4$, and $\text{SNR}_{\text{UL}} = \text{SNR}_{\text{DL}} = 10$ dB.

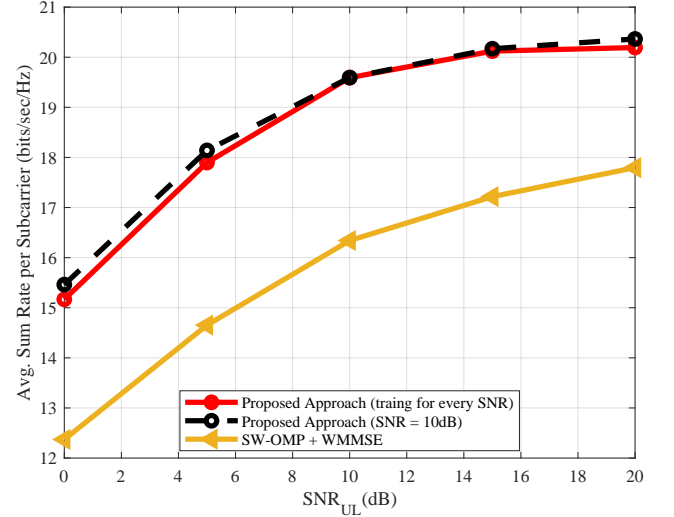
To ensure that the number of RF chains is always equal to the number of users, we select only K RF chains for downlink precoding. This assumption is needed for the proposed scheme as well as the PM design. In both cases, we observe that the proposed approach provides better performance than the channel recovery based approaches, regardless of the number of users.

D. System-Level Performance

The simulation results presented so far pertains to the sum rate objective. To evaluate the system-level performance of the proposed algorithm and to account for fairness across the users, we examine the performance of the proposed approach in an urban micro cell with 200 meters radius and 2000 potential users. The users are placed randomly in a circular region within distances between 30 to 200 meters from the

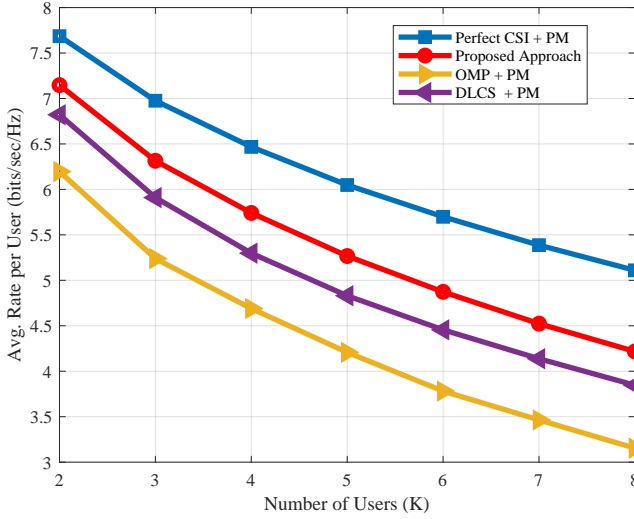


(a) Generalizability in the number of paths for the proposed scheme. We fix $\text{SNR}_{\text{UL}} = 10$ dB, and vary L_p from 2 to 8 paths.

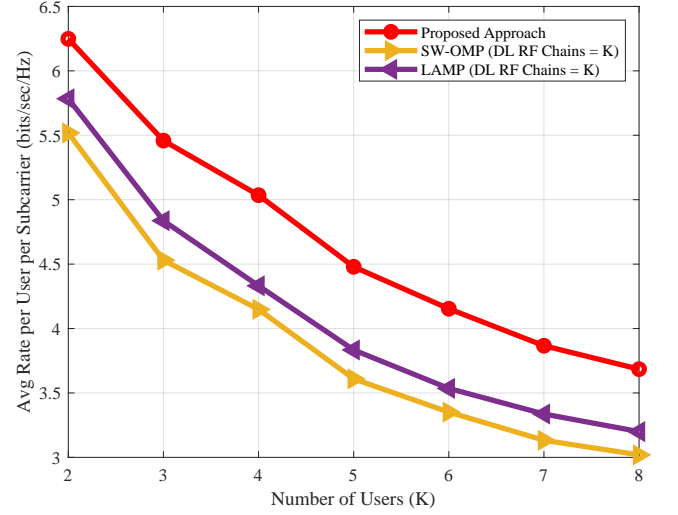


(b) Generalizability in the uplink SNR for the proposed scheme. We fix $L_p = 4$, and vary SNR_{UL} from 0 to 20 dB.

Fig. 8: Generalizability of the multi-carrier DNN in environment parameters. We set $N_{\text{RF}} = K = 4$, and $\text{SNR}_{\text{DL}} = 10$ dB.



(a) single-carrier system



(b) Multi-carrier system

Fig. 9: Generalizability in the number of users. Here, we set $N_{\text{RF}} = 8$ and vary K from 2 to 8 users.

BS. The antenna gain and transmit power at the BS are 0dBi and 40dBm. Similarly, the antenna gain and transmit power at the users are 15dBi and 30dBm. Further, it is assumed that the users experience both large-scale fading and small-scale fading. The small-scale fading component follows the frequency-selective mmWave model presented in Section II-B with $L_p = 4$, whereas the large-scale fading component follows the floating intercept model derived in [37] from 38 GHz empirical measurements. The cell allocated bandwidth is 10MHz and the noise spectral density is -173.8 dBm/Hz.

We assume that communication occurs in a time slotted fashion. In each time slot, $N_{\text{RF}} = K = 4$ users are scheduled randomly. Further, we consider weighted sum rate as the metric of performance, where the weights are inversely proportional to the long term average of the scheduled users' rates in previous time slots in order to maximize the log utility. For the proposed design, we choose $L_a = 10$ and $L_d = 4$, and

set $L = 14$ for the other precoding schemes. Moreover, for the analog part design we train one SU-DNN (using the loss function in (25)) on a training set sampled randomly from the channel distributions of all users in the cell. After that, we evaluate the performance using 4 identical copies of the trained DNN. Finally, we use WMMSE to design the digital part for both the proposed as well as the baseline approaches.

Fig. 10 shows the empirical cumulative distribution function (CDF) of the average rate per users for different hybrid precoding schemes. It can be observed that the average user rate under the proposed scheme is much higher than the average user rate under the channel recovery based precoding schemes. This suggests that the SU-DNN with sufficient complexity can generally learn a good mapping for the analog part design despite being trained under vastly different channel conditions. In other words, sharing the weights across the branches of the DNN architecture can still ensure a generalizability in the

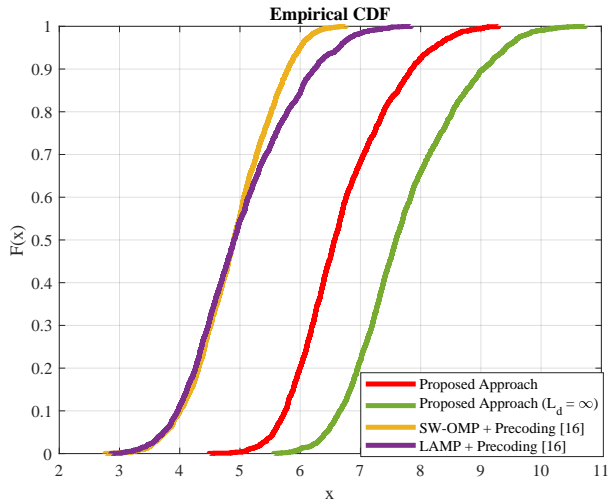


Fig. 10: Empirical CDF of the average user rate under different hybrid precoding schemes in an urban cell scenario. We set $M = 64$, $N_{\text{RF}} = K = 4$, $L_a = 10$, $L_d = 4$, and $L = 14$.

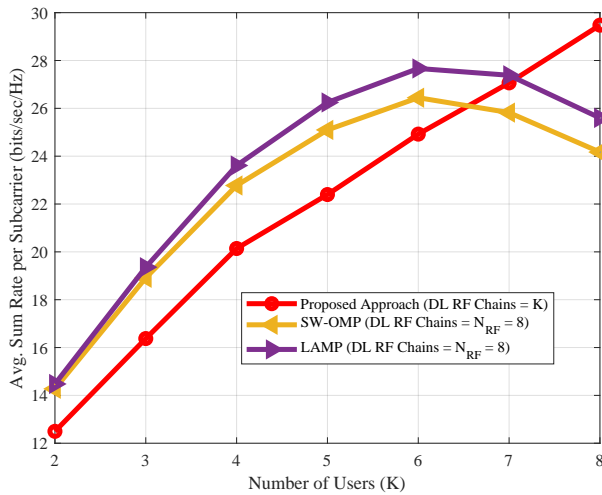


Fig. 11: Performance of the proposed scheme when $N_{\text{RF}} \geq K$. We set $M = 64$ and $L = 7$, with $L_a = 5$ and $L_d = 2$.

number of users even when the users do not share the same channel distribution. Moreover, the superior performance of the proposed scheme suggests its suitability for maximizing not only the sum rate but a more general network utility function (e.g., weighted sum rate). This fact can be seen by noting that the loss function in (19) (or the more general variant (25)) can be regarded as a universally good measure of performance for the analog part design since it encourages the analog beamformer phases to match to the channel phases, while allowing the subsequent digital precoder to alleviate the inter-user interference. Finally, comparing the CDF curves of the proposed approach when $L_a = 10$ and $L_d = \infty$ indicates that the proposed design can be further improved by employing longer L_d .

E. Performance when $N_{\text{RF}} > K$

As a final simulation, we investigate the performance of the proposed approach when the number of RF chains exceeds the number of users. To this end, we fix $N_{\text{RF}} = 8$ and plot the performance for different values of $K \leq 8$. We remark here

that because of our initial assumption that $N_{\text{RF}} = K$, we can only utilize K out of N_{RF} RF chains for downlink precoding using the proposed design. In contrast, the channel recovery based approaches can utilize all N_{RF} RF chains for downlink precoding since the covariance based approach [16] does not require this assumption. Fig. 11 shows the comparison for different precoding schemes. We observe that the proposed scheme can eventually outperform the channel recovery based approaches when the system is fully loaded, but it achieves a lower sum rate when $K < N_{\text{RF}}$. This is because the channel recovery based schemes can take advantage of the increased degrees of freedom (offered by utilizing all N_{RF} chains) when the number of users is small. This is a limitation of the proposed scheme. However, in practice, network operators typically set $N_{\text{RF}} \approx K$ to ensure that the system is working near the fully loaded regime, which is exactly the scenario where the proposed approach has significant advantage over the channel recovery based counterparts.

VI. CONCLUSION

This paper addresses the design of hybrid analog and digital precoding matrices in a mmWave TDD massive MIMO employing single-carrier or multi-carrier transmission techniques. The proposed learning based precoding strategy overcomes the limitations of the existing schemes by constructing the analog precoding matrices directly from the received pilots without the intermediate step of estimating the high dimensional channel. Further, the design of the digital precoding follows from estimating a low-dimensional equivalent channel using a relatively small number of pilots. In contrast to the fully direct approach of jointly learning the analog and digital precoding matrices, the proposed approach significantly simplifies the training process and can generalize to systems with an arbitrary number of users. Numerical evaluations indicate significant gains in spectral efficiency relative to the channel recovery based schemes and further demonstrate the ability of the proposed scheme to generalize in various system parameters.

REFERENCES

- [1] K. M. Attiah, F. Sahrabi, and W. Yu, "Deep learning approach to channel sensing and hybrid precoding for TDD massive MIMO systems," in *IEEE Global Commun. (GLOBECOM) Workshop*, Taipei, Taiwan, Dec. 2020.
- [2] S. Rangan, T. S. Rappaport, and E. Erkip, "Millimeter-wave cellular wireless networks: Potentials and challenges," *Proc. IEEE*, vol. 102, no. 3, pp. 366–385, Mar. 2014.
- [3] R. W. Heath, N. González-Prelcic, S. Rangan, W. Roh, and A. M. Sayeed, "An overview of signal processing techniques for millimeter wave MIMO systems," *IEEE J. Sel. Topics Signal Process.*, vol. 10, no. 3, pp. 436–453, Apr. 2016.
- [4] P. Wang, Y. Li, L. Song, and B. Vucetic, "Multi-gigabit millimeter wave wireless communications for 5G: From fixed access to cellular networks," *IEEE Commun. Mag.*, vol. 53, no. 1, pp. 168–178, Jan. 2015.
- [5] T. L. Marzetta, "Noncooperative cellular wireless with unlimited numbers of base station antennas," *IEEE Trans. Wireless Commun.*, vol. 9, no. 11, pp. 3590–3600, Nov. 2010.
- [6] X. Zhang, A. F. Molisch, and S.-Y. Kung, "Variable-phase-shift-based RF-baseband codesign for MIMO antenna selection," *IEEE Trans. Signal Process.*, vol. 53, no. 11, pp. 4091–4103, Oct. 2005.
- [7] O. El Ayach, S. Rajagopal, S. Abu-Surra, Z. Pi, and R. Heath, "Spatially sparse precoding in millimeter wave MIMO systems," *IEEE Trans. Wireless Commun.*, vol. 13, no. 3, pp. 1499–1513, Mar. 2014.

- [8] J. Lee, G. Gil, and Y. H. Lee, "Channel estimation via orthogonal matching pursuit for hybrid MIMO systems in millimeter wave communications," *IEEE Trans. Commun.*, vol. 64, no. 6, pp. 2370–2386, June 2016.
- [9] A. Alkhateeb, O. El Ayach, G. Leus, and R. Heath, "Channel estimation and hybrid precoding for millimeter wave cellular systems," *IEEE J. Sel. Topics Signal Process.*, vol. 8, no. 5, pp. 831–846, Oct. 2014.
- [10] F. Bellili, F. Sofrabi, and W. Yu, "Generalized approximate message passing for massive MIMO mmWave channel estimation with Laplacian prior," *IEEE Trans. Commun.*, vol. 67, no. 5, pp. 3205–3219, May 2019.
- [11] J. Rodríguez-Fernández, N. González-Prelcic, K. Venugopal, and R. W. Heath, "Frequency-domain compressive channel estimation for frequency-selective hybrid millimeter wave MIMO systems," *IEEE Trans. Wireless Commun.*, vol. 17, no. 5, pp. 2946–2960, May 2018.
- [12] A. Li and C. Masouros, "Hybrid precoding and combining design for millimeter-wave multi-user MIMO based on SVD," in *IEEE Int. Conf. Commun. (ICC)*, Paris, France, May 2017, pp. 1–6.
- [13] L. Liang, W. Xu, and X. Dong, "Low-complexity hybrid precoding in massive multiuser MIMO systems," *IEEE Wireless Commun. Lett.*, vol. 3, no. 6, pp. 653–656, Dec. 2014.
- [14] L. Liang, Y. Dai, W. Xu, and X. Dong, "How to approach zero-forcing under RF chain limitations in large mmwave multiuser systems?" in *IEEE Int. Conf. Commun. China (ICCC)*, Shanghai, China, Oct. 2014, pp. 518–522.
- [15] F. Sofrabi and W. Yu, "Hybrid digital and analog beamforming design for large-scale antenna arrays," *IEEE J. Sel. Topics Signal Process.*, vol. 10, no. 3, pp. 501–513, Jan. 2016.
- [16] F. Sofrabi and W. Yu, "Hybrid analog and digital beamforming for mmwave OFDM large-scale antenna arrays," *IEEE J. Sel. Areas Commun.*, vol. 35, no. 7, pp. 1432–1443, July 2017.
- [17] S. Park, A. Alkhateeb, and R. W. Heath, "Dynamic subarrays for hybrid precoding in wideband mmwave MIMO systems," *IEEE Trans. Wireless Commun.*, vol. 16, no. 5, pp. 2907–2920, May 2017.
- [18] S. Payami, M. Sellathurai, and K. Nikitopoulos, "Low-complexity hybrid beamforming for massive MIMO systems in frequency-selective channels," *IEEE Access*, vol. 7, pp. 36 195–36 206, Mar. 2019.
- [19] X. Yu, J.-C. Shen, J. Zhang, and K. B. Letaief, "Alternating minimization algorithms for hybrid precoding in millimeter wave MIMO systems," *IEEE J. Sel. Topics Signal Process.*, vol. 10, no. 3, pp. 485–500, Apr. 2016.
- [20] Z. Gao, C. Hu, L. Dai, and Z. Wang, "Channel estimation for millimeter-wave massive MIMO with hybrid precoding over frequency-selective fading channels," *IEEE Commun. Lett.*, vol. 20, no. 6, pp. 1259–1262, Apr. 2016.
- [21] F. Sofrabi, Z. Chen, and W. Yu, "Deep active learning approach to adaptive beamforming for mmwave initial alignment," *IEEE J. Sel. Areas Commun.*, vol. 39, no. 8, pp. 2347–2360, Aug. 2021.
- [22] M. Borgerding, P. Schniter, and S. Rangan, "AMP-inspired deep networks for sparse linear inverse problems," *IEEE Trans. Signal Process.*, vol. 65, no. 16, pp. 4293–4308, Aug. 2017.
- [23] X. Ma, Z. Gao, F. Gao, and M. Di Renzo, "Model-driven deep learning based channel estimation and feedback for millimeter-wave massive hybrid MIMO systems," *IEEE J. Sel. Areas Commun.*, vol. 39, no. 8, pp. 2388–2406, Aug. 2021.
- [24] T. Lin and Y. Zhu, "Beamforming design for large-scale antenna arrays using deep learning," *IEEE Wireless Commun. Lett.*, vol. 9, no. 1, pp. 103–107, Jan. 2020.
- [25] A. M. Elbir and A. K. Papazafeiropoulos, "Hybrid precoding for multiuser millimeter wave massive MIMO systems: A deep learning approach," *IEEE Trans. Veh. Technol.*, vol. 69, no. 1, pp. 552–563, Jan. 2020.
- [26] W. Ma, C. Qi, Z. Zhang, and J. Cheng, "Sparse channel estimation and hybrid precoding using deep learning for millimeter wave massive MIMO," *IEEE Trans. Commun.*, vol. 68, no. 5, pp. 2838–2849, Jan. 2020.
- [27] W. Cui, K. Shen, and W. Yu, "Spatial deep learning for wireless scheduling," *IEEE J. Sel. Areas Commun.*, vol. 37, no. 6, pp. 1248–1261, June 2019.
- [28] T. Jiang, H. V. Cheng, and W. Yu, "Learning to reflect and to beamform for intelligent reflecting surface with implicit channel estimation," *IEEE J. Sel. Areas Commun.*, vol. 39, no. 7, pp. 1931–1945, July 2021.
- [29] F. Sofrabi, K. M. Attiah, and W. Yu, "Deep learning for distributed channel feedback and multiuser precoding in FDD massive MIMO," *IEEE Trans. Wireless Commun.*, vol. 20, no. 7, pp. 4044–4057, July 2021.
- [30] A. M. Elbir, K. V. Mishra, M. Shankar, and B. Ottersten, "A family of deep learning architectures for channel estimation and hybrid beamforming in multi-carrier mm-Wave massive MIMO," Dec. 2019. [Online]. Available: <https://arxiv.org/abs/1912.10036>
- [31] G. S. Smith, "A direct derivation of a single-antenna reciprocity relation for the time domain," *IEEE Trans. Antennas Propag.*, vol. 52, no. 6, pp. 1568–1577, June 2004.
- [32] A. Alkhateeb, "DeepMIMO: A generic deep learning dataset for millimeter wave and massive MIMO applications," in *Proc. Inf. Theory Appl. Workshop (ITA)*, San Diego, CA, Feb 2019, pp. 1–8.
- [33] X. Sun, C. Qi, and G. Y. Li, "Beam training and allocation for multiuser millimeter wave massive MIMO systems," *IEEE Trans. Wireless Commun.*, vol. 18, no. 2, pp. 1041–1053, Feb. 2019.
- [34] Q. Shi, M. Razaviyayn, Z.-Q. Luo, and C. He, "An iteratively weighted MMSE approach to distributed sum-utility maximization for a MIMO interfering broadcast channel," *IEEE Trans. Signal Process.*, vol. 59, no. 9, pp. 4331–4340, Sept. 2011.
- [35] M. Abadi et al., "TensorFlow: Large-scale machine learning on heterogeneous distributed systems," Mar. 2016. [Online]. Available: <https://arxiv.org/abs/1603.04467>
- [36] D. P. Kingma and J. Ba, "Adam: A method for stochastic optimization," Dec. 2014. [Online]. Available: <https://arxiv.org/abs/1412.6980>
- [37] G. R. MacCartney, J. Zhang, S. Nie, and T. S. Rappaport, "Path loss models for 5G millimeter wave propagation channels in urban microcells," in *IEEE Global Commun. (GLOBECOM)*, June 2013, pp. 3948–3953.